Simultaneous extraction of transversity and Collins functions from new semi-inclusive deep inelastic scattering and e^{+}e^{-} data

M. Anselmino, M. Boglione, U. D'Alesio, S. Melis, F. Murgia, and A. Prokudin

Phys. Rev. D **87**, 094019 — Published 17 May 2013

DOI: 10.1103/PhysRevD.87.094019

Simultaneous extraction of transversity and Collins functions from new SIDIS and e^+e^- data

M. Anselmino,[1,2] M. Boglione,[1,2] U. D'Alesio,[3,4] S. Melis,[1,2] F. Murgia,[4] and A. Prokudin[5]

[1] *Dipartimento di Fisica, Università di Torino, Via P. Giuria 1, I-10125 Torino, Italy*
[2] *INFN, Sezione di Torino, Via P. Giuria 1, I-10125 Torino, Italy*
[3] *Dipartimento di Fisica, Università di Cagliari, Cittadella Universitaria, I-09042 Monserrato (CA), Italy*
[4] *INFN, Sezione di Cagliari, C.P. 170, I-09042 Monserrato (CA), Italy*
[5] *Jefferson Laboratory, 12000 Jefferson Avenue, Newport News, VA 23606, USA*

We present a global re-analysis of the most recent experimental data on azimuthal asymmetries in semi-inclusive deep inelastic scattering, from the HERMES and COMPASS Collaborations, and in $e^+e^- \to h_1\, h_2\, X$ processes, from the Belle Collaboration. The transversity and the Collins functions are extracted simultaneously, in the framework of a revised analysis in which a new parameterisation of the Collins functions is also tested.

PACS numbers: 13.88.+e, 13.60.-r, 13.66.Bc, 13.85.Ni

I. INTRODUCTION AND FORMALISM

The spin structure of the nucleon, in its partonic collinear configuration, is fully described, at leading-twist, by three independent Parton Distribution Functions (PDFs): the unpolarised PDF, the helicity distribution and the transversity distribution. While the unpolarised PDF and the helicity distribution, which have been studied for decades, are by now very well or reasonably well known, much less information is available on the latter, which has been studied only recently. The reason is that, due to its chiral-odd nature, a transversity distribution can only be accessed in processes where it couples to another chiral-odd quantity.

The chiral-odd partner of the transversity distribution could be a fragmentation function, like the Collins function [1] or the di-hadron fragmentation function [2–4] or another parton distribution, like the Boer-Mulders [5] or the transversity distribution itself. A chiral-odd partonic distribution couples to a chiral-odd fragmentation function in Semi-Inclusive Deep Inelastic Scattering processes (SIDIS, $\ell\, N \to \ell\, h\, X$). The coupling of two chiral-odd partonic distributions could occur in Drell-Yan processes (D-Y, $h\, N \to \ell^+\ell^-\, X$) but, so far, no data on polarised D-Y is available. Information on the convolution of two chiral-odd fragmentation functions (FFs) can be obtained from $e^+e^- \to h_1\, h_2\, X$ processes.

The u and d quark transversity distributions, together with the Collins fragmentation functions, have been extracted for the first time in Refs. [6, 7], from a combined analysis of SIDIS and e^+e^- data. Similar results on the transversity distributions, coupled to the di-hadron, rather than the Collins, fragmentation function, have been obtained recently [8]. These independent results establish with certainty the role played by the transversity distributions in SIDIS azimuthal asymmetries.

Since the first papers [6, 7], new data have become available: from the COMPASS experiment operating on a transversely polarised proton (NH_3 target) [9, 10], from a final analysis of the HERMES Collaboration [11] and from corrected results of the Belle Collaboration [12]. This fresh information motivates a new global analysis for the simultaneous extraction of the transversity distributions and the Collins functions.

This is performed using techniques similar to those implemented in Refs. [6, 7]; in addition, a second, different parameterisation of the Collins function will be tested, in order to assess the influence of a particular functional form on our results.

Let us briefly recall the strategy followed and the formalism adopted in extracting the transversity and Collins distribution functions from independent SIDIS and e^+e^- data.

A. SIDIS

We consider, at $\mathcal{O}(k_\perp/Q)$, the SIDIS process $\ell\, p^\uparrow \to \ell'\, h\, X$ and the single spin asymmetry,

$$A_{UT}^{\sin(\phi_h+\phi_S)} = 2\, \frac{\int d\phi_h\, d\phi_S\, [d\sigma^\uparrow - d\sigma^\downarrow]\, \sin(\phi_h+\phi_S)}{\int d\phi_h\, d\phi_S\, [d\sigma^\uparrow + d\sigma^\downarrow]}\,, \tag{1}$$

where $d\sigma^{\uparrow,\downarrow}$ is a shorthand notation for

$$d\sigma^{\uparrow,\downarrow} \equiv \frac{d^6\sigma^{\ell p^{\uparrow,\downarrow}\to\ell h X}}{dx\,dy\,dz\,d^2\boldsymbol{P}_T\,d\phi_S}$$

and x, y, z are the usual SIDIS variables:

$$x = x_{_B} = \frac{Q^2}{2(P\cdot q)} \qquad y = \frac{(P\cdot q)}{(P\cdot \ell)} = \frac{Q^2}{x\,s} \qquad z = z_h = \frac{(P\cdot P_h)}{(P\cdot q)}\,. \tag{2}$$

We adopt here the same notations and kinematical variables as defined in Refs. [6, 13], to which we refer for further details, in particular for the definition of the azimuthal angles which appear above and in the following equations.

By considering the $\sin(\phi_h+\phi_S)$ moment of A_{UT} [14], we are able to single out the effect originating from the spin dependent part of the fragmentation function of a transversely polarised quark, embedded in the Collins function, $\Delta^N D_{h/q^\uparrow}(z,p_\perp) = (2\,p_\perp/z\,m_h)\,H_1^{\perp q}(z,p_\perp)$ [15], coupled to the TMD transversity distribution $\Delta_T q(x,k_\perp)$ [6]:

$$A_{UT}^{\sin(\phi_h+\phi_S)} = \frac{\displaystyle\sum_q e_q^2 \int d\phi_h\,d\phi_S\,d^2\boldsymbol{k}_\perp\,\Delta_T q(x,k_\perp)\,\frac{d(\Delta\hat\sigma)}{dy}\,\Delta^N D_{h/q^\uparrow}(z,p_\perp)\sin(\phi_S+\varphi+\phi_q^h)\sin(\phi_h+\phi_S)}{\displaystyle\sum_q e_q^2 \int d\phi_h\,d\phi_S\,d^2\boldsymbol{k}_\perp\,f_{q/p}(x,k_\perp)\,\frac{d\hat\sigma}{dy}\;D_{h/q}(z,p_\perp)}\,, \tag{3}$$

where $\boldsymbol{p}_\perp = \boldsymbol{P}_T - z\boldsymbol{k}_\perp$, and

$$\frac{d\hat\sigma}{dy} = \frac{2\pi\alpha^2}{sxy^2}[1+(1-y)^2] \qquad \frac{d(\Delta\hat\sigma)}{dy} \equiv \frac{d\hat\sigma^{\ell q^\uparrow\to\ell q^\uparrow}}{dy} - \frac{d\hat\sigma^{\ell q^\uparrow\to\ell q^\downarrow}}{dy} = \frac{4\pi\alpha^2}{sxy^2}(1-y)\,. \tag{4}$$

The usual integrated transversity distribution is given, according to some common notations, by:

$$\Delta_T q(x) \equiv h_{1q}(x) = \int d^2\boldsymbol{k}_\perp\,\Delta_T q(x,k_\perp)\,. \tag{5}$$

This analysis, performed at $\mathcal{O}(k_\perp/Q)$, can be further simplified adopting a Gaussian and factorized parameterisation of the TMDs. In particular for the unpolarized parton distribution (TMD-PDFs) and fragmentation (TMD-FFs) functions we use:

$$f_{q/p}(x,k_\perp) \;=\; f_{q/p}(x)\,\frac{e^{-k_\perp^2/\langle k_\perp^2\rangle}}{\pi\langle k_\perp^2\rangle} \tag{6}$$

$$D_{h/q}(z,p_\perp) \;=\; D_{h/q}(z)\,\frac{e^{-p_\perp^2/\langle p_\perp^2\rangle}}{\pi\langle p_\perp^2\rangle}\,, \tag{7}$$

with $\langle k_\perp^2\rangle$ and $\langle p_\perp^2\rangle$ fixed to the values found in Ref. [16] by analyzing unpolarized SIDIS azimuthal dependent data:

$$\langle k_\perp^2\rangle = 0.25\ \text{GeV}^2 \qquad \langle p_\perp^2\rangle = 0.20\ \text{GeV}^2\,. \tag{8}$$

The integrated parton distribution and fragmentation functions, $f_{q/p}(x)$ and $D_{h/q}(z)$, are available in the literature; in particular, we use the GRV98LO PDF set [17] and the DSS fragmentation function set [18].

For the transversity distribution, $\Delta_T q(x,k_\perp)$, and the Collins FF, $\Delta^N D_{h/q^\uparrow}(z,p_\perp)$, we adopt the following parameterisations [6]:

$$\Delta_T q(x,k_\perp) \;=\; \frac{1}{2}\,\mathcal{N}_q^T(x)\,[f_{q/p}(x)+\Delta q(x)]\,\frac{e^{-k_\perp^2/\langle k_\perp^2\rangle_T}}{\pi\langle k_\perp^2\rangle_T} \tag{9}$$

$$\Delta^N D_{h/q^\uparrow}(z,p_\perp) \;=\; 2\,\mathcal{N}_q^C(z)\,D_{h/q}(z)\,h(p_\perp)\,\frac{e^{-p_\perp^2/\langle p_\perp^2\rangle}}{\pi\langle p_\perp^2\rangle}\,, \tag{10}$$

with

$$\mathcal{N}_q^T(x) = N_q^T\;x^\alpha(1-x)^\beta\,\frac{(\alpha+\beta)^{(\alpha+\beta)}}{\alpha^\alpha\beta^\beta} \tag{11}$$

$$\mathcal{N}_q^C(z) = N_q^C\;z^\gamma(1-z)^\delta\,\frac{(\gamma+\delta)^{(\gamma+\delta)}}{\gamma^\gamma\delta^\delta} \tag{12}$$

$$h(p_\perp) = \sqrt{2e}\,\frac{p_\perp}{M_h}\,e^{-p_\perp^2/M_h^2}\,, \tag{13}$$

and $-1 \leq N_q^T \leq 1$, $-1 \leq N_q^C \leq 1$. We assume $\langle k_\perp^2 \rangle_{_T} = \langle k_\perp^2 \rangle$. The combination $[f_{q/p}(x) + \Delta q(x)]$, where $\Delta q(x)$ is the helicity distribution, is evolved in Q^2 according to Ref. [19]. Notice that with these choices both the transversity and the Collins function automatically obey their proper positivity bounds. A different functional form of $\mathcal{N}_q^C(z)$ will be explored in Section II B.

Using these parameterisations we obtain the following expression for $A_{UT}^{\sin(\phi_h+\phi_S)}$:

$$A_{UT}^{\sin(\phi_h+\phi_S)} = \frac{\dfrac{P_T}{M_h}\,\dfrac{1-y}{sxy^2}\,\sqrt{2e}\,\dfrac{\langle p_\perp^2\rangle_C^2}{\langle p_\perp^2\rangle}\,\dfrac{e^{-P_T^2/\langle P_T^2\rangle_C}}{\langle P_T^2\rangle_C^2}\displaystyle\sum_q e_q^2\,\mathcal{N}_q^T(x)\,\big[f_{q/p}(x)+\Delta q(x)\big]\;\mathcal{N}_q^C(z)\,D_{h/q}(z)}{\dfrac{e^{-P_T^2/\langle P_T^2\rangle}}{\langle P_T^2\rangle}\,\dfrac{[1+(1-y)^2]}{sxy^2}\displaystyle\sum_q e_q^2\,f_{q/p}(x)\;D_{h/q}(z)}\,, \tag{14}$$

with

$$\langle p_\perp^2\rangle_C = \frac{M_h^2\,\langle p_\perp^2\rangle}{M_h^2+\langle p_\perp^2\rangle} \qquad \langle P_T^2\rangle_{(C)} = \langle p_\perp^2\rangle_{(C)} + z^2\langle k_\perp^2\rangle\,. \tag{15}$$

When data or phenomenological information at different Q^2 values are considered, we take into account, at leading order (LO), the QCD evolution of the integrated transversity distribution. For the Collins FF, $\Delta^N D_{h/q^\uparrow}$, as its scale dependence is unknown, we tentatively assume the same Q^2 evolution as for the unpolarized FF, $D_{h/q}(z)$.

B. $e^+e^- \to h_1 h_2\, X$ processes

Remarkably, independent information on the Collins functions can be obtained in unpolarized e^+e^- processes, by looking at the azimuthal correlations of hadrons produced in opposite jets [20]. This has been performed by the Belle Collaboration, which have measured azimuthal hadron-hadron correlations for inclusive charged pion production, $e^+e^- \to \pi\,\pi\,X$ [12, 21, 22]. This correlation can be interpreted as a direct measure of the Collins effect, involving the convolution of two Collins functions.

Two methods have been adopted in the experimental analysis of the Belle data. These can be schematically described as (for further details and definitions see Refs. [6, 20, 22]):
i) the "$\cos(\varphi_1+\varphi_2)$ method" in the Collins-Soper frame where the jet thrust axis is used as the $\hat{z}$ direction and the $e^+e^- \to q\,\bar{q}$ scattering defines the $\widehat{xz}$ plane; φ_1 and φ_2 are the azimuthal angles of the two hadrons around the thrust axis;
ii) the "$\cos(2\varphi_0)$ method", using the Gottfried-Jackson frame where one of the produced hadrons (h_2) identifies the $\hat{z}$ direction and the $\widehat{xz}$ plane is determined by the lepton and the h_2 directions. There will then be another relevant plane, determined by $\hat{z}$ and the direction of the other observed hadron h_1, at an angle φ_0 with respect to the $\widehat{xz}$ plane.

In both cases one integrates over the magnitude of the intrinsic transverse momenta of the hadrons with respect to the fragmenting quarks. For the $\cos(\varphi_1+\varphi_2)$ method the cross section for the process $e^+e^- \to h_1\,h_2\,X$ reads:

$$\begin{aligned}
&\frac{d\sigma^{e^+e^-\to h_1h_2X}}{dz_1\,dz_2\,d\cos\theta\,d(\varphi_1+\varphi_2)}\\
&= \frac{3\alpha^2}{4s}\sum_q e_q^2\Big\{(1+\cos^2\theta)\,D_{h_1/q}(z_1)\,D_{h_2/\bar{q}}(z_2)\\
&+ \frac{\sin^2\theta}{4}\,\cos(\varphi_1+\varphi_2)\,\Delta^N D_{h_1/q^\uparrow}(z_1)\,\Delta^N D_{h_2/\bar{q}^\uparrow}(z_2)\Big\}\,,
\end{aligned} \tag{16}$$

where θ is the angle between the lepton direction and the thrust axis and

$$\Delta^N D_{h/q^\uparrow}(z) \equiv \int d^2\boldsymbol{p}_\perp \Delta^N D_{h/q^\uparrow}(z,p_\perp)\,. \tag{17}$$

Integrating over the covered values of θ and normalizing to the corresponding azimuthal averaged unpolarized cross section one has:

$$R_{12}(z_1,z_2,\varphi_1+\varphi_2) \equiv \frac{1}{\langle d\sigma\rangle}\,\frac{d\sigma^{e^+e^-\to h_1h_2X}}{dz_1\,dz_2\,d(\varphi_1+\varphi_2)}$$

$$= 1 + \frac{1}{4}\,\frac{\langle \sin^2\theta\rangle}{\langle 1+\cos^2\theta\rangle}\,\cos(\varphi_1+\varphi_2)\,\frac{\sum_q e_q^2\,\Delta^N D_{h_1/q^\uparrow}(z_1)\,\Delta^N D_{h_2/\bar q^\uparrow}(z_2)}{\sum_q e_q^2\,D_{h_1/q}(z_1)\,D_{h_2/\bar q}(z_2)} \tag{18}$$

$$\equiv 1 + \frac{1}{4}\,\frac{\langle \sin^2\theta\rangle}{\langle 1+\cos^2\theta\rangle}\,\cos(\varphi_1+\varphi_2)\,P(z_1,z_2)\,.$$

For the $\cos(2\varphi_0)$ method, with the Gaussian ansatz (10), the analogue of Eq. (18) reads

$$R_0(z_1,z_2,\varphi_0) \equiv \frac{1}{\langle d\sigma\rangle}\,\frac{d\sigma^{e^+e^-\to h_1h_2X}}{dz_1\,dz_2\,d\varphi_0}$$

$$= 1 + \frac{1}{\pi}\,\frac{z_1\,z_2}{z_1^2+z_2^2}\,\frac{\langle \sin^2\theta_2\rangle}{\langle 1+\cos^2\theta_2\rangle}\,\cos(2\varphi_0)\,\frac{\sum_q e_q^2\,\Delta^N D_{h_1/q^\uparrow}(z_1)\,\Delta^N D_{h_2/\bar q^\uparrow}(z_2)}{\sum_q e_q^2 D_{h_1/q}(z_1)\,D_{h_2/\bar q}(z_2)} \tag{19}$$

$$\equiv 1 + \frac{1}{\pi}\,\frac{z_1\,z_2}{z_1^2+z_2^2}\,\frac{\langle \sin^2\theta_2\rangle}{\langle 1+\cos^2\theta_2\rangle}\,\cos(2\varphi_0)\,P(z_1,z_2)\,,$$

where θ_2 is now the angle between the lepton and the h_2 hadron directions.

In both cases, Eqs. (18) and (19), the value of

$$\frac{\langle \sin^2\theta\rangle}{\langle 1+\cos^2\theta\rangle} \equiv C(\theta) \tag{20}$$

can be found in the experimental data (see Tables IV and V of Ref. [22]).

To eliminate false asymmetries, the Belle Collaboration consider the ratio of unlike-sign ($\pi^+\pi^- + \pi^-\pi^+$) to like-sign ($\pi^+\pi^+ + \pi^-\pi^-$) or charged ($\pi^+\pi^+ + \pi^+\pi^- + \pi^-\pi^+ + \pi^-\pi^-$) pion pair production, denoted respectively with indices U, L and C. For example, in the case of unlike- to like-pair production, one has

$$\frac{R_{12}^U}{R_{12}^L} = \frac{1+\frac{1}{4}\,C(\theta)\,\cos(\varphi_1+\varphi_2)\,P_U}{1+\frac{1}{4}\,C(\theta)\,\cos(\varphi_1+\varphi_2)\,P_L} \;\simeq\; 1+\frac{1}{4}\,C(\theta)\cos(\varphi_1+\varphi_2)\,(P_U-P_L) \tag{21}$$

$$\equiv\; 1+\cos(\varphi_1+\varphi_2)\,A_{12}^{UL} \tag{22}$$

and

$$\frac{R_0^U}{R_0^L} = \frac{1+\frac{1}{\pi}\,\frac{z_1\,z_2}{z_1^2+z_2^2}\,C(\theta)\,\cos(2\varphi_0)\,P_U}{1+\frac{1}{\pi}\,\frac{z_1\,z_2}{z_1^2+z_2^2}\,C(\theta)\,\cos(2\varphi_0)\,P_L} \;\simeq\; 1+\frac{1}{\pi}\,\frac{z_1\,z_2}{z_1^2+z_2^2}\,C(\theta)\cos(2\varphi_0)\,(P_U-P_L) \tag{23}$$

$$\equiv\; 1+\cos(2\varphi_0)\,A_0^{UL} \tag{24}$$

and similarly for R_{12}^U/R_{12}^C and R_0^U/R_0^C. Explicitely, one has:

$$P_U = \frac{\sum_q e_q^2\,[\Delta^N D_{\pi^+/q^\uparrow}(z_1)\,\Delta^N D_{\pi^-/\bar q^\uparrow}(z_2) + \Delta^N D_{\pi^-/q^\uparrow}(z_1)\,\Delta^N D_{\pi^+/\bar q^\uparrow}(z_2)]}{\sum_q e_q^2\,[D_{\pi^+/q}(z_1)\,D_{\pi^-/\bar q}(z_2) + D_{\pi^-/q}(z_1)\,D_{\pi^+/\bar q}(z_2)]} \equiv \frac{(P_U)_N}{(P_U)_D} \tag{25}$$

$$P_L = \frac{\sum_q e_q^2\,[\Delta^N D_{\pi^+/q^\uparrow}(z_1)\,\Delta^N D_{\pi^+/\bar q^\uparrow}(z_2) + \Delta^N D_{\pi^-/q^\uparrow}(z_1)\,\Delta^N D_{\pi^-/\bar q^\uparrow}(z_2)]}{\sum_q e_q^2\,[D_{\pi^+/q}(z_1)\,D_{\pi^+/\bar q}(z_2) + D_{\pi^-/q}(z_1)\,D_{\pi^-/\bar q}(z_2)]} \equiv \frac{(P_L)_N}{(P_L)_D} \tag{26}$$

$$P_C = \frac{(P_U)_N + (P_L)_N}{(P_U)_D + (P_L)_D} \tag{27}$$

$$A_{12}^{UL,C}(z_1,z_2) = \frac{1}{4}\,\frac{\langle \sin^2\theta\rangle}{\langle 1+\cos^2\theta\rangle}\,(P_U - P_{L,C}) \tag{28}$$

$$A_0^{UL,C}(z_1,z_2) = \frac{1}{\pi}\,\frac{z_1\,z_2}{z_1^2+z_2^2}\,\frac{\langle \sin^2\theta_2\rangle}{\langle 1+\cos^2\theta_2\rangle}\,(P_U - P_{L,C})\,. \tag{29}$$

For fitting purposes, it is convenient to introduce favoured and disfavoured fragmentation functions, assuming in Eq. (10):

$$\frac{\Delta^N D_{\pi^+/u^\uparrow,\bar d^\uparrow}(z,p_\perp)}{D_{\pi^+/u,\bar d}(z)} = \frac{\Delta^N D_{\pi^-/d^\uparrow,\bar u^\uparrow}(z,p_\perp)}{D_{\pi^-/d,\bar u}(z)} = 2\,\mathcal{N}_{\rm fav}^C(z)\,h(p_\perp)\,\frac{e^{-p_\perp^2/\langle p_\perp^2\rangle}}{\pi\langle p_\perp^2\rangle} \tag{30}$$

TABLE I: Summary of the χ^2 values obtained in our fits. The columns, from left to right give the χ^2 per degree of freedom, the total χ^2, and the separate contributions to the total χ^2 of the data from SIDIS, A_{12}^{UL}, A_{12}^{UC}, A_0^{UL} and A_0^{UC}. "NO FIT" means that the χ^2 for that set of data does not refer to a best fit, but to the computation of the corresponding quantity using the best fit parameters fixed by the other data. The four lines show the results for the two choices of parameterisation of the z dependence of the Collins functions (standard and polynomial) and for the two independent sets of data fitted (SIDIS, A_{12}^{UL}, A_{12}^{UC} and SIDIS, A_0^{UL}, A_0^{UC}).

	FIT DATA 178 points	SIDIS 146 points	A_{12}^{UL} 16 points	A_{12}^{UC} 16 points	A_0^{UL} 16 points	A_0^{UC} 16 points
Standard Parameterisation $\chi^2_{\rm d.o.f} = 0.80$	$\chi^2_{\rm tot} = 135$	$\chi^2 = 123$	$\chi^2 = 7$	$\chi^2 = 5$	$\chi^2 = 44$ NO FIT	$\chi^2 = 39$ NO FIT
Standard Parameterisation $\chi^2_{\rm d.o.f} = 1.12$	$\chi^2_{\rm tot} = 190$	$\chi^2 = 125$	$\chi^2 = 20$ NO FIT	$\chi^2 = 12$ NO FIT	$\chi^2 = 35$	$\chi^2 = 30$
Polynomial Parameterisation $\chi^2_{\rm d.o.f} = 0.81$	$\chi^2_{.\rm tot} = 136$	$\chi^2 = 123$	$\chi^2 = 8$	$\chi^2 = 5$	$\chi^2 = 45$ NO FIT	$\chi^2 = 39$ NO FIT
Polynomial Parameterisation $\chi^2_{\rm d.o.f} = 1.01$	$\chi^2_{\rm tot} = 171$	$\chi^2 = 141$	$\chi^2 = 44$ NO FIT	$\chi^2 = 27$ NO FIT	$\chi^2 = 15$	$\chi^2 = 15$

$$\frac{\Delta^N D_{\pi^+/d^\uparrow,\bar{u}^\uparrow}(z,p_\perp)}{D_{\pi^+/d,\bar{u}}(z)} = \frac{\Delta^N D_{\pi^-/u^\uparrow,\bar{d}^\uparrow}(z,p_\perp)}{D_{\pi^-/u,\bar{d}}(z)} = \frac{\Delta^N D_{\pi^\pm/s^\uparrow,\bar{s}^\uparrow}(z,p_\perp)}{D_{\pi^\pm/s,\bar{s}}(z)} = 2\,\mathcal{N}^C_{\rm dis}(z)\,h(p_\perp)\,\frac{e^{-p_\perp^2/\langle p_\perp^2\rangle}}{\pi\langle p_\perp^2\rangle}\,, \qquad (31)$$

with the corresponding relations for the integrated Collins functions, Eq. (17), and with $\mathcal{N}^C_{\rm fav,dis}(z)$ as given in Eq. (12) with $N_q^C = N^C_{\rm fav,dis}$.

We can now perform a best fit of the data from HERMES and COMPASS on $A_{UT}^{\sin(\phi_h+\phi_S)}$ and of the data, from the Belle Collaboration, on $A_{12}^{UL,C}$ and $A_0^{UL,C}$. Their expressions, Eqs. (14) and (25)–(31), contain the transversity and the Collins functions, parameterised as in Eqs. (9)–(13). They depend on the free parameters $\alpha, \beta, \gamma, \delta, N_q^T, N_q^C$ and M_h. Following Ref. [6] we assume the exponents α, β and the mass scale M_h to be flavour independent and consider the transversity distributions only for u and d quarks (with the two free parameters N_u^T and N_d^T). The favoured and disfavoured Collins functions are fixed, in addition to the flavour independent exponents γ and δ, by $N^C_{\rm fav}$ and $N^C_{\rm dis}$. This makes a total of 9 parameters, to be fixed with a best fit procedure. Notice that while in the present analysis we can safely neglect any flavour dependence of the parameter β (which is anyway hardly constrained by the SIDIS data), this issue could play a significant role in other studies, like those discussed in Ref. [23].

II. BEST FITS, RESULTS AND PARAMETERISATIONS

A. Standard parameterisation

We start by repeating the same fitting procedure as in Refs. [6, 7], using the same "standard" parameterisation, Eqs. (6)–(13), with the difference that now we include all the most recent SIDIS data from COMPASS [10] and HERMES [11] Collaborations, and the corrected Belle data [12] on A_{12}^{UL} and A_{12}^{UC}. Notice, in particular, that the A_{12}^{UC} data are included in our fits for the first time here. In fact, a previous inconsistency between A_{12}^{UL} and A_{12}^{UC} data, present in the first Belle results [21], has been removed in Ref. [12].

The results we obtain are remarkably good, with a total $\chi^2_{\rm d.o.f}$ of 0.80, as reported in the first line of Table I, and the values of the resulting parameters, given in Table II, are consistent with those found in our previous extractions. Our best fits are shown in Fig. 1 (upper plots), for the Belle A_{12} data, in Fig. 2 for the SIDIS COMPASS data and in Fig. 3 for the HERMES results.

We have not inserted the A_0 Belle data in our global analysis as they are strongly correlated with the A_{12} results, being a different analysis of the same experimental events. However, using the extracted parameters we can compute the A_0^{UL} and A_0^{UC} azimuthal asymmetries, in good qualitative agreement with the Belle measurements, although the corresponding χ^2 values are rather large, as shown in Table I. These results are presented in Fig. 1 (lower plots).

The shaded uncertainty bands are computed according to the procedure explained in the Appendix of Ref. [24]. We have allowed the set of best fit parameters to vary in such a way that the corresponding new curves have a total χ^2 which differs from the best fit χ^2 by less than a certain amount $\Delta\chi^2$. All these (1500) new curves lie inside the shaded area. The chosen value of $\Delta\chi^2 = 17.21$ is such that the probability to find the "true" result inside the shaded band is 95.45%.

We have also performed a global fit based on the SIDIS and A_0 Belle data, and then computed the A_{12} values. We do not show the best fit plots, which are not very informative, but the quality of the results can be judged from the second line of Table I, which shows that although this time A_0^{UL} and A_0^{UC} are actually fitted, their corresponding χ^2 values remain large. This has induced us to explore a different functional shape for the parameterisation of $\mathcal{N}_q^C(z)$, Eq. (12), which will be discussed in the next Subsection.

The difference between A_{12} and A_0 is a delicate issue, that deserves some further comments. On the experimental side, the hadronic-plane method used for the extraction of A_0 implies a simple analysis of the raw data, as it requires the sole reconstruction of the tracks of the two detected hadrons; therefore it leads to very clean data points, with remarkably small error bars. On the contrary, the thrust-axis method is much more involved as it requires the reconstruction of the original direction of the q and $\bar{q}$ which fragment into the observed hadrons; this makes the measurement of the A_{12} asymmetry experimentally more challenging, and leads to data points whith larger uncertainties.

On the theoretical side, the situation is just the opposite: as the thrust-axis method assumes a perfect knowledge of the q and $\bar{q}$ directions, the asymmetry can be reconstructed by a straightforward integration over the two intrinsic transverse momenta $p_{\perp 1}$ and $p_{\perp 2}$, transforming the convolution of two Collins functions into the much simpler product of two Collins moments [6], Eqs. (17) and (18). Instead, the phenomenological partonic expression of A_0 involves more complicated kinematical relations and some approximations; the simple final outcome, Eq. (19), holds at $\mathcal{O}(k_\perp/z\sqrt{s})$ and $(p_\perp/P)$ (where P is the final hadron 3-momentum magnitude) [6]. Thus, on the theoretical side, the partonic interpretation of A_0 is a bit less clean.

One should also add that most of the large χ^2 values found when computing A_0 from the parameters of a best fit involving SIDIS and A_{12} data (or vice-versa) originate from the experimental points at large values of z_1 or z_2 or both (see, for example the last points on the left lower panel in Fig. 1). Large values of z bring us near the exclusive process limit, where our factorized inclusive approach cannot hold anymore.

B. Polynomial parameterisation

In an attempt to fit equally well A_{12} and A_0 (keeping in mind, however, the comments at the end of the previous Subsection) we have explored a possible new parameterisation of the z dependence of the Collins function. We notice that data on $A_0(z)$ seem to favour an increase at large z values, rather then a decrease, which is implicitly forced by a behaviour of the kind given in Eqs. (10) and (12) (at least with positive δ values).

In addition, an increasing trend of $A_0(z)$ and $A_{12}(z)$ seems to be confirmed by very interesting preliminary results of the BABAR Collaboration, which have performed an independent new analysis of $e^+e^- \to h_1\, h_2\, X$ data [25], analogous to that of Belle.

TABLE II: Best values of the 9 free parameters fixing the u and d quark transversity distribution functions and the favoured and disfavoured Collins fragmentation functions, as obtained by fitting simultaneously SIDIS data on the Collins asymmetry and Belle data on A_{12}^{UL} and A_{12}^{UC}. The transversity distributions are parameterised according to Eqs. (9), (11) and the Collins fragmentation functions according to the standard parameterisation, Eqs. (10), (12) and (13). We obtain a total χ^2/d.o.f. = 0.80. The statistical errors quoted for each parameter correspond to the shaded uncertainty areas in Figs. 1–3, as explained in the text and in the Appendix of Ref. [24].

$N_u^T = 0.46^{+0.20}_{-0.14}$	$N_d^T = -1.00^{+1.17}_{-0.00}$
$\alpha = 1.11^{+0.89}_{-0.66}$	$\beta = 3.64^{+5.80}_{-3.37}$
$N_{\rm fav}^C = 0.49^{+0.20}_{-0.18}$	$N_{\rm dis}^C = -1.00^{+0.38}_{-0.00}$
$\gamma = 1.06^{+0.45}_{-0.32}$	$\delta = 0.07^{+0.42}_{-0.07}$
$M_h^2 = 1.50^{+2.00}_{-1.12}$ GeV^2	

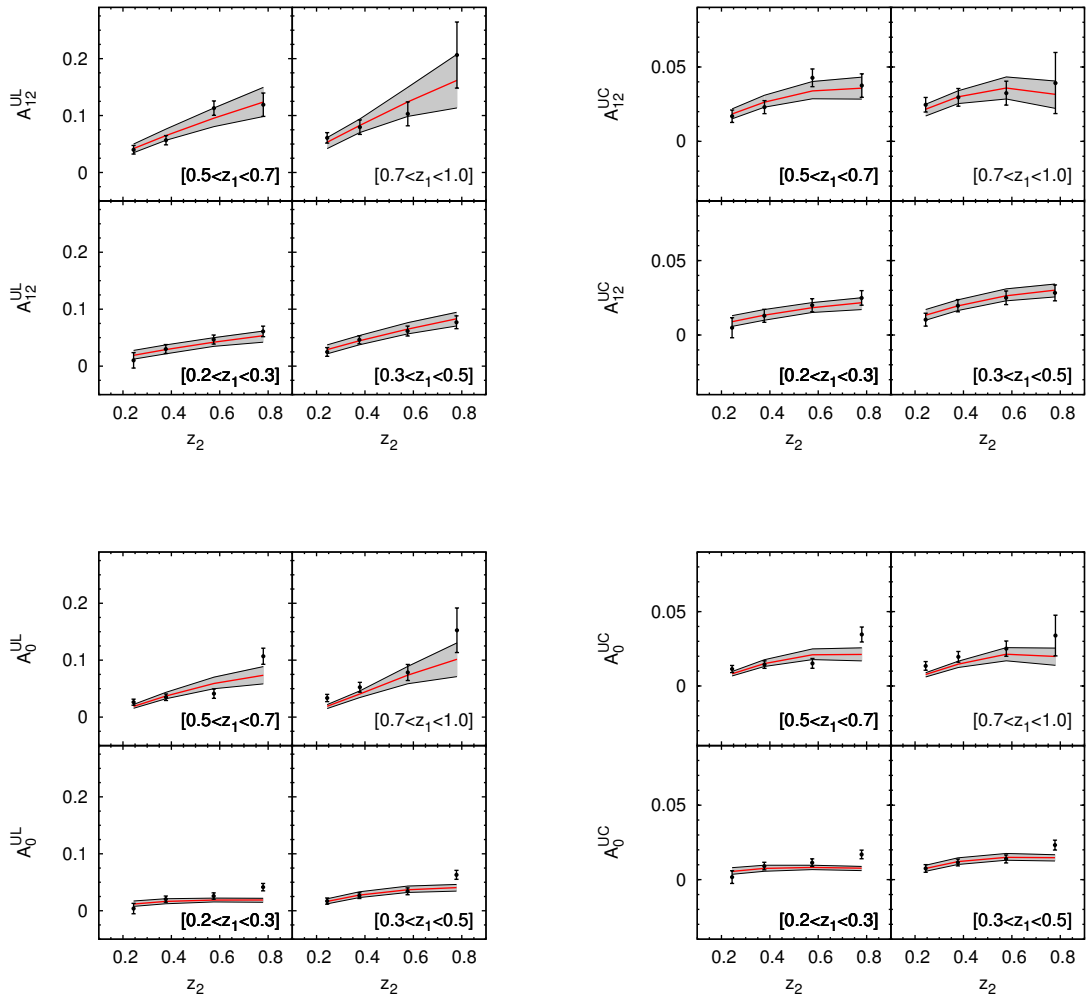

FIG. 1: The experimental data on A_{12}^{UL}, A_{12}^{UC} (upper plots) and A_0^{UL} and A_0^{UC} (lower plots), as measured by the Belle Collaboration [12] in unpolarized $e^+e^- \to h_1\, h_2\, X$ processes, are compared to the curves obtained from our global fit. The solid lines correspond to the parameters given in Table II, obtained by fitting the SIDIS and the A_{12} asymmetries with the standard parameterisation; the shaded areas correspond to the statistical uncertainty on the parameters, as explained in the text and in Ref. [24]. Notice that the A_0^{UL} and A_0^{UC} data are not included in the fit and our curves, with the corresponding uncertainties, are simply computed using the parameters of Table II.

This suggests that a different parameterisation of the z dependence of favoured and disfavoured Collins functions could turn out to be more convenient. Then, we try an alternative polynomial parameterisation which allows more flexibility on the behaviour of $\mathcal{N}_q^C(z)$ at large z:

$$\mathcal{N}_q^C(z) = N_q^C\; z\,[(1-a-b) + a\,z + b\,z^2]\,, \tag{32}$$

with the subfix $q = \text{fav}, \text{dis}$, and $-1 \le N_q^C \le 1$; a and b are flavour independent so that the total number of parameters for the Collins functions (in addition to M_h) remains 4. Such a choice fixes the term $\mathcal{N}_q^C(z)$ to be equal to 0 at $z = 0$ and not larger than 1 at $z = 1$. Notice that we do not automatically impose, as in Eq. (12), the condition $|\mathcal{N}_q^C(z)| \le 1$; however, we have explicitly checked that the best fit results and all the sets of parameters corresponding to curves inside the shaded uncertainty bands satisfy that condition.

We have repeated the same fitting procedure as performed with the standard parameterisation. When fitting the combined SIDIS, A_{12}^{UL} and A_{12}^{UC} Belle data, the resulting best fits (not shown) hardly exhibit any difference with respect to those obtained with the standard parameterisation (Fig. 1). This can be seen also from the χ^2's in Table I, where the third line is very similar to the first one. As a further confirmation, the corresponding best fit plots for $\mathcal{N}_{\text{fav,dis}}^C(z)$, in case of the standard and polynomial parameterisations, plotted in Fig. 4 (left panel) practically coincide

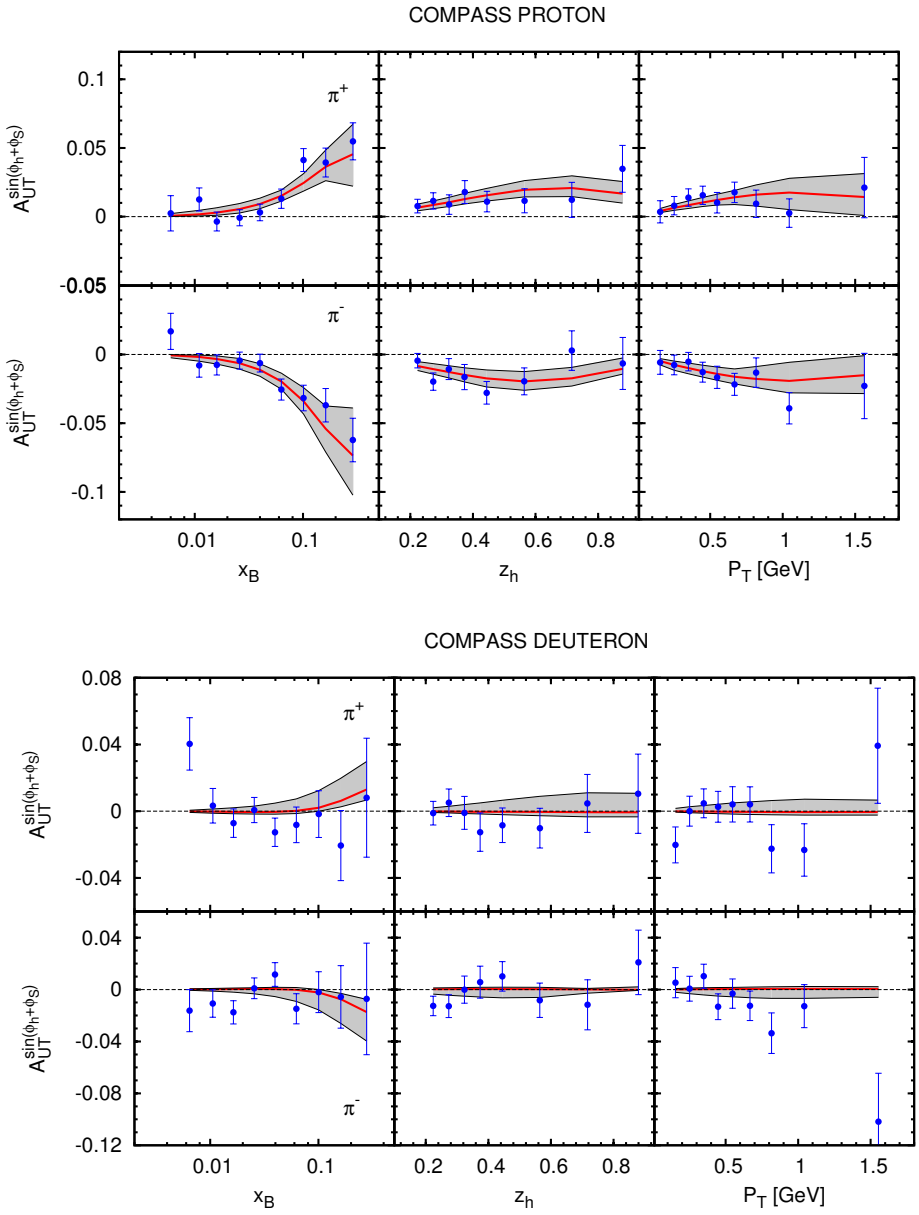

FIG. 2: The experimental data on the SIDIS azimuthal moment $A_{UT}^{\sin(\phi_h+\phi_S)}$ as measured by the COMPASS Collaboration [10] on proton (upper plots) and deuteron (lower plots) targets, are compared to the curves obtained from our global fit. The solid lines correspond to the parameters given in Table II, obtained by fitting the SIDIS and the A_{12} asymmetries with standard parameterisation; the shaded areas correspond to the statistical uncertainty on the parameters, as explained in the text and in Ref. [24].

up to values of z very close to 1.

The situation is different when best fitting the SIDIS data together with A_0^{UL} and A_0^{UC}; in such a case the polynomial parameterisation allows a much better best fit, as shown in Fig. 5, upper plots. A reasonable agreement can also be achieved between the data and the computed values of A_{12}^{UL} and A_{12}^{UC}, as shown by the χ^2 values in Table I and by the lower plots in Fig. 5. In this case the polynomial form of $\mathcal{N}^C_{\rm fav,dis}(z)$ differs from the standard one, as shown in the right plots in Fig. 4.

Notice, again, that the large χ^2 values of the computed A_{12}^{UL} is almost completely due to the last z bins, which correspond to the quasi exclusive region. Also, the larger χ^2 values corresponding to SIDIS data are mainly due to a slightly worse description of HERMES π^- azimuthal moments. The values of the parameters obtained using the

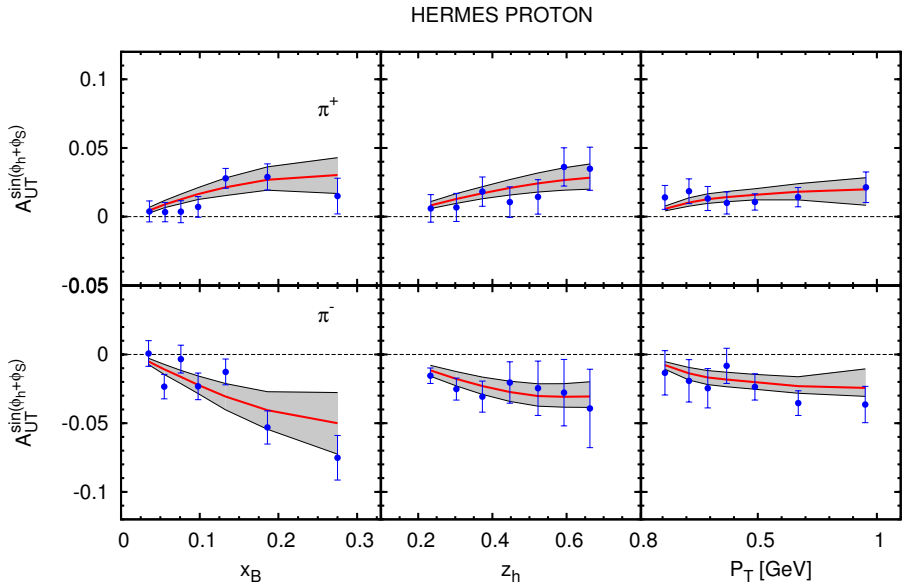

FIG. 3: The experimental data on the SIDIS azimuthal moment $A_{UT}^{\sin(\phi_h+\phi_S)}$ as measured by the HERMES Collaboration [11], are compared to the curves obtained from our global fit. The solid lines correspond to the parameters given in Table II, obtained by fitting the SIDIS and the A_{12} asymmetries with standard parameterisation; the shaded areas correspond to the statistical uncertainty on the parameters, as explained in the text and in Ref. [24].

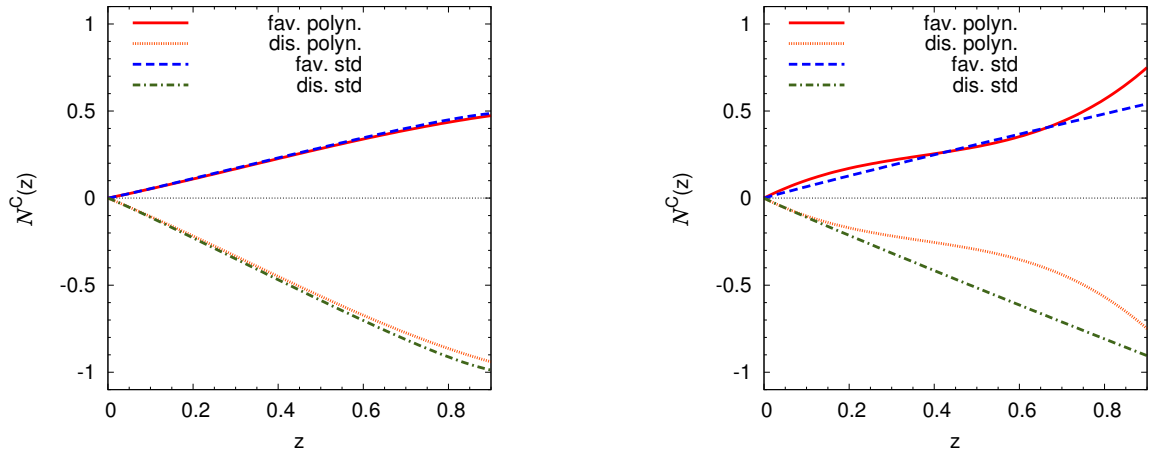

FIG. 4: Plots of the functions $\mathcal{N}^C_{\rm fav}(z)$ and $\mathcal{N}^C_{\rm dis}(z)$ for the favoured and disfavoured Collins functions as obtained by using the standard, Eq. (12), and polynomial, Eq. (32), parameterisations. On the left panel we show the results obtained by fitting the SIDIS data together with the A_{12} Belle asymmetries (both with standard and polynomial parameterisation), while on the right panel we show the corresponding results obtained by fitting the SIDIS data together with the A_0 Belle asymmetries.

polynomial shape of $\mathcal{N}^C_{\rm fav,dis}(z)$, Eq. (32), are given in Table III.

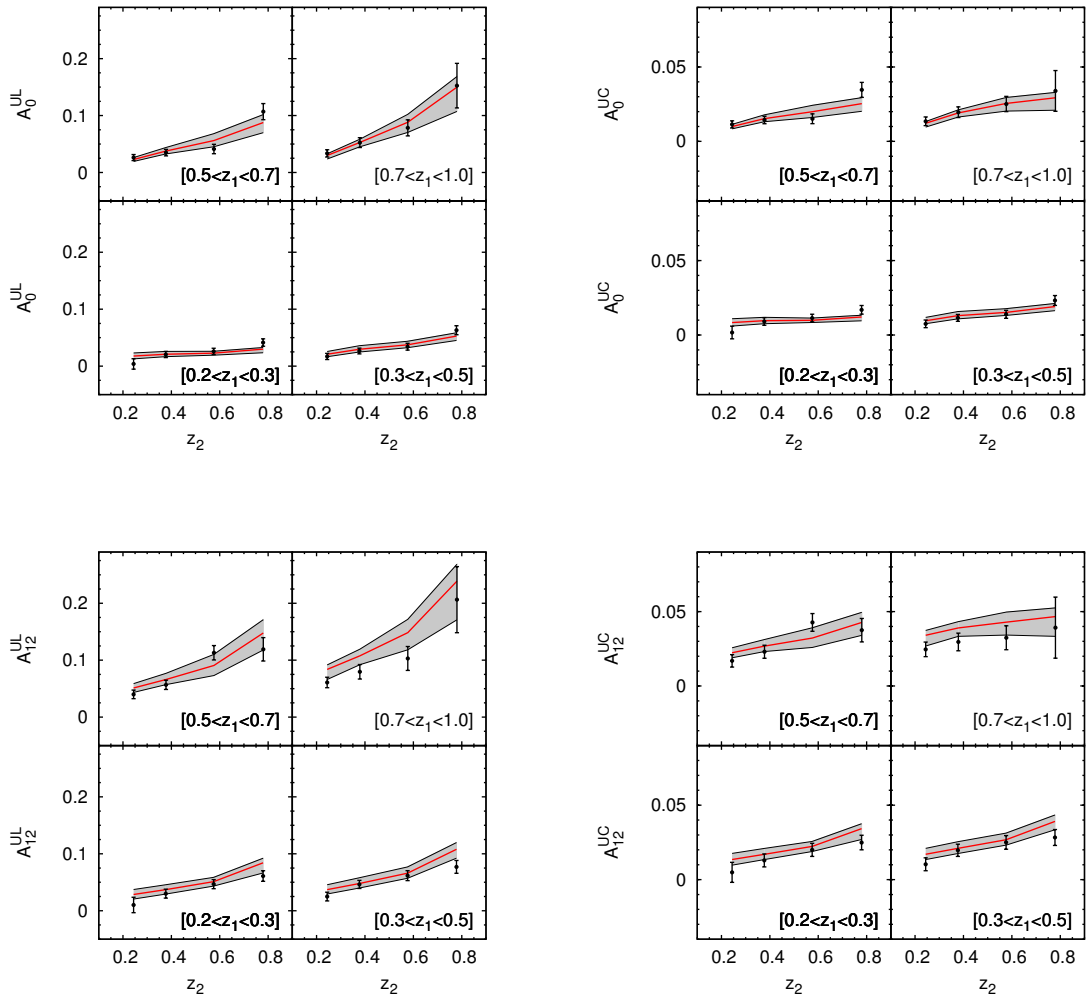

FIG. 5: The experimental data on A_0^{UL}, A_0^{UC} (upper plots) and A_{12}^{UL} and A_{12}^{UC} (lower plots), as measured by the Belle Collaboration [12] in unpolarized $e^+e^- \to h_1\, h_2\, X$ processes, are compared to the curves obtained from our global fit. The solid lines correspond to the parameters given in Table III, obtained by fitting the SIDIS and the A_0 asymmetries with polynomial parameterisation; the shaded areas correspond to the statistical uncertainty on the parameters, as explained in the text and in Ref. [24]. Notice that the A_{12}^{UL} and A_{12}^{UC} data are not included in the fit and our curves, with the corresponding uncertainties, are simply computed using the parameters of Table III.

C. The extracted transversity and Collins functions; predictions and final comments

Our newly extracted transversity and Collins functions are shown in Figs. 6 and 7; to be precise, in the left panels we show $x\,\Delta_T q(x) = x\,h_{1q}(x)$, for u and d quarks, while in the right panels we plot:

$$z\,\Delta^N D_{h/q^\uparrow}(z) = z\int d^2\boldsymbol{p}_\perp \Delta^N D_{h/q^\uparrow}(z,p_\perp) = z\int d^2\boldsymbol{p}_\perp \frac{2\,p_\perp}{z\,m_h}\,H_1^{\perp q}(z,p_\perp) = 4z\,H_1^{\perp(1/2)q}(z) \tag{33}$$

for $h = \pi^\pm$ and $q = u$. The Collins results for d quark are not shown explicitly, but could be obtained from Tables II and III.

Fig. 6 shows the results which best fit the COMPASS and HERMES SIDIS data on $A_{UT}^{\sin(\phi_h+\phi_S)}$, together with the Belle results on A_{12}^{UL} and A_{12}^{UC}, using the standard parameterisation. The red solid lines correspond to the parameters given in Table II. The shaded bands show the uncertainty region, which is the region spanned by the 1500 different sets of parameters fixed according to the procedure explained above and in the Appendix of Ref. [24]. The blue dashed lines show, for comparison, our previous results [7]: the difference between the solid red and dashed blue lines is only due to the updated SIDIS and A_{12}^{UL} data used here, with the addition of A_{12}^{UC}, while keeping the same

TABLE III: Best values of the 9 free parameters fixing the u and d quark transversity distribution functions and the favoured and disfavoured Collins fragmentation functions, as obtained by fitting simultaneously SIDIS data on the Collins asymmetry and Belle data on A_0^{UL} and A_0^{UC}. The transversity distributions are parameterised according to Eqs. (9), (11) and the Collins fragmentation functions according to the polynomial parameterisation, Eqs. (10), (32) and (13). We obtain a total χ^2/d.o.f. = 1.01. The statistical errors quoted for each parameter correspond to the shaded uncertainty areas in Fig. 5, as explained in the text and in the Appendix of Ref. [24].

$N_u^T = 0.36^{+0.19}_{-0.12}$	$N_d^T = -1.00^{+0.40}_{0.00}$
$\alpha = 1.06^{+0.87}_{-0.56}$	$\beta = 3.66^{+5.87}_{-2.78}$
$N^C_{\rm fav} = 1.00^{+0.00}_{-0.36}$	$N^C_{\rm dis} = -1.00^{+0.19}_{-0.00}$
$a = -2.36^{+1.24}_{-0.98}$	$b = 2.12^{+0.61}_{-1.12}$
$M_h^2 = 0.67^{+1.09}_{-0.36}$ GeV^2	

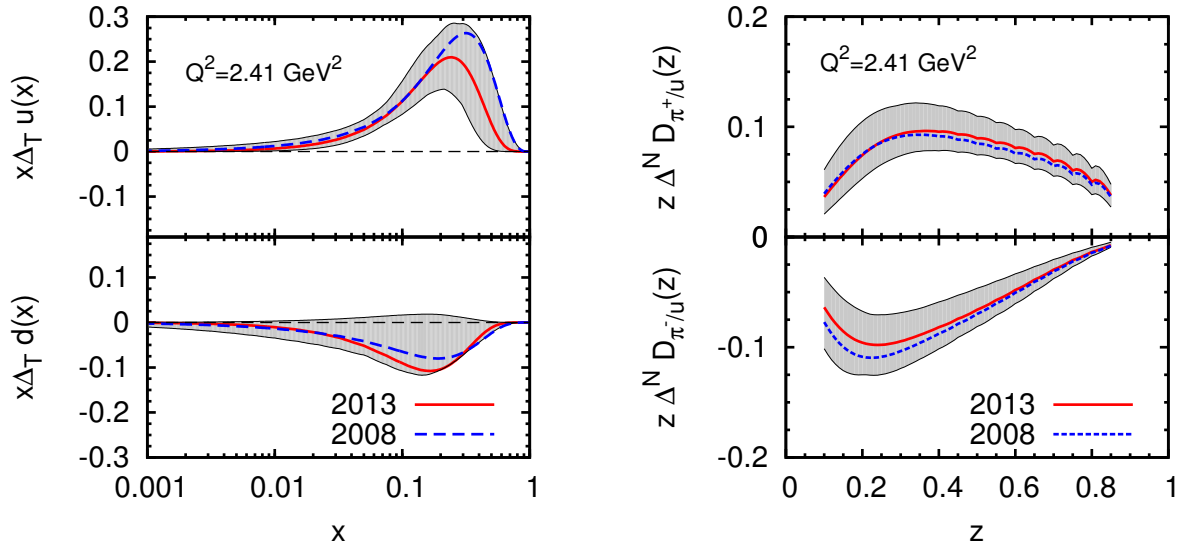

FIG. 6: The left panel shows (solid red lines) the transversity distribution functions $x\,h_{1q}(x) = x\,\Delta_T q(x)$ for $q = u, d$, with their uncertainty bands (shaded areas), obtained from the best fit of SIDIS data on $A_{UT}^{\sin(\phi_h+\phi_S)}$ and e^+e^- data on A_{12}, adopting the standard parameterisation (Table II). Similarly, the right panel shows the corresponding first moment of the favoured and disfavoured Collins functions, Eq. (33). All results are given at $Q^2 = 2.41$ GeV^2. The corresponding results using the polynomial parameterisation, not shown, would almost entirely overlap with those shown here, both for the transversity and the Collins functions. The dashed blue lines show the same quantities as obtained in Ref. [7] using the data then available on $A_{UT}^{\sin(\phi_h+\phi_S)}$ and A_{12}^{UL}.

parameterisation. The present and previous results agree within the uncertainty band: one could at most notice a slight decrease of the new u quark transversity distribution at large x values.

Fig. 7 shows the results which best fit the COMPASS and HERMES SIDIS data on $A_{UT}^{\sin(\phi_h+\phi_S)}$, together with the Belle results on A_0^{UL} and A_0^{UC}, using the polynomial parameterisation. The red solid lines correspond to the parameters given in Table III. This is not a simple updating of our previous 2008 fit [7], as we use different sets of data (SIDIS and A_0 rather than SIDIS and A_{12}) with a different polynomial parameterisation. In this case the comparison with the 2008 results is less significant. When comparing the results of Fig. 6 and 7, one notices a sizeable difference in the favoured (u/π^+) Collins function, and less evident differences in the transversity distributions.

In Fig. 8 we show, for comparison with similar results presented in Ref. [7], the tensor charge, corresponding to our best fit transversity distributions, as given in Tables II and III. Our extracted values are shown at $Q^2 = 0.8$ GeV^2 and compared with several model computations. One should keep in mind that our estimates are based on the

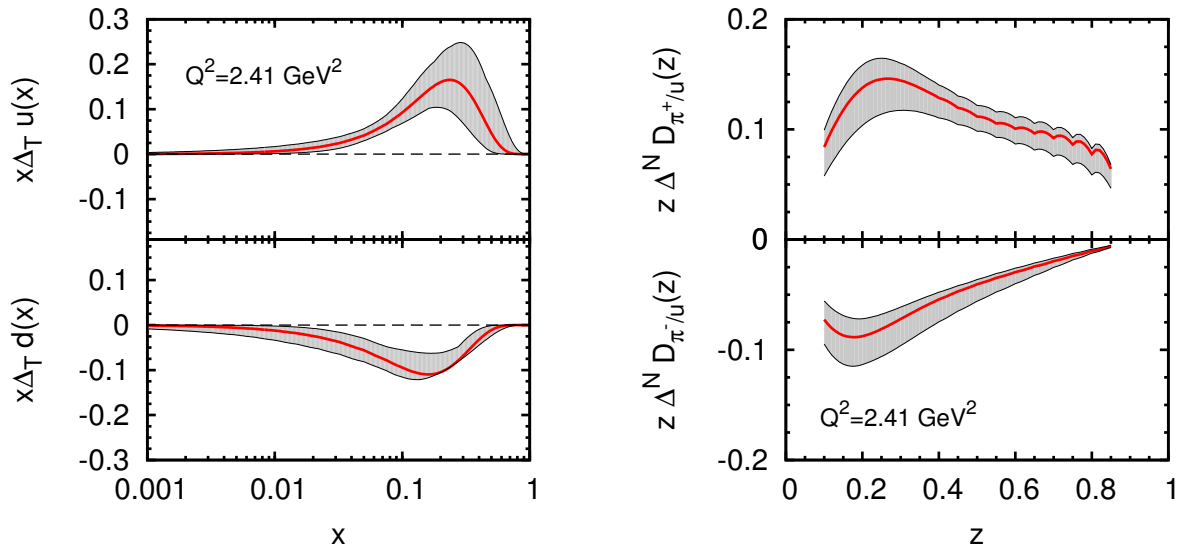

FIG. 7: The left panel shows (solid red lines) the transversity distribution functions $x\,h_{1q}(x) = x\,\Delta_T q(x)$ for $q = u, d$, with their uncertainty bands (shaded areas), obtained from our best fit of SIDIS data on $A_{UT}^{\sin(\phi_h+\phi_S)}$ and e^+e^- data on A_0, adopting the polynomial parameterisation (Table III). Similarly, the right panel shows the corresponding first moment of the favoured and disfavoured Collins functions, Eq. (33). All results are given at $Q^2 = 2.41$ GeV^2. The corresponding results using the standard parameterisation, not shown, would almost entirely overlap with those shown here for the transversity distribution. The favoured Collins function would be smaller and the disfavoured one also smaller (*i.e.* larger in magnitude), with their uncertainty bands still partially overlapping.

assumption of a negligible contribution from sea quarks and on a set of data which still cover a limited range of x values.

All other results are shown at the scale $Q^2 = 2.41$ GeV^2. The evolution to the chosen value has been obtained by evolving at LO the collinear part of the factorized distribution and fragmentation functions. The TMD evolution, which might affect the $k_\perp$ and $p_\perp$ dependence, is not yet known for the Collins function. Consistently, it has not been taken into account for the other distribution and fragmentation functions.

We have not included in our fit some recent results on the SIDIS Collins asymmetry on a neutron target published by the Jefferson Lab Hall A Collaboration at 6 GeV [33]. These results have been obtained from data (4 points) off a ^{3}He target, and the extraction of $A_{UT}^{\sin(\phi_h+\phi_S)}$ for a neutron requires some model dependence in order to take into account nuclear effects; the published results have indeed large errors. If we use our extracted transversity distributions and Collins functions, exploiting isospin symmetry and the same model [34] for the nuclear effects as in Ref. [33], we find a negligible Collins asymmetry on a ^{3}He target, which is in agreement with 3 out of the 4 data points of JLab.

As BABAR data on A_{12} and A_0 should be available soon, we show in Figs. 9 and 10 our expectations, based on our extracted Collins functions. Fig. 9 shows the expected values of A_{12}^{UL}, A_{12}^{UC}, A_0^{UL} and A_0^{UC}, as a function of z_2 for different bins of z_1, using the parameters of Table II, obtained by fitting the SIDIS and the A_{12} Belle data with the standard parameterisation. Fig. 10 shows the same quantities using the parameters of Table III, obtained by fitting the SIDIS and the A_0 Belle data with the polynomial parameterisation.

The Belle (and BABAR) e^+e^- results on the azimuthal correlations of hadrons produced in opposite jets, together with the SIDIS data on the azimuthal asymmetry $A_{UT}^{\sin(\phi_h+\phi_S)}$, measured by both the HERMES and COMPASS Collaborations, definitely establish the importance of the Collins effect in the fragmentation of a transversely polarised quark. In addition, the SIDIS asymmetry can only be observed if coupled to a non negligible quark transversity distribution. The first original extraction of the transversity distribution and the Collins fragmentation functions [6, 7], has been confirmed here, with new data and a possible new functional shape of the Collins functions. The results on the transversity distribution have also been confirmed independently in Ref. [8].

A further improvement in the QCD analysis of the experimental data, towards a more complete understanding of the Collins and transversity distributions, and their possible role in other processes, would require taking into account

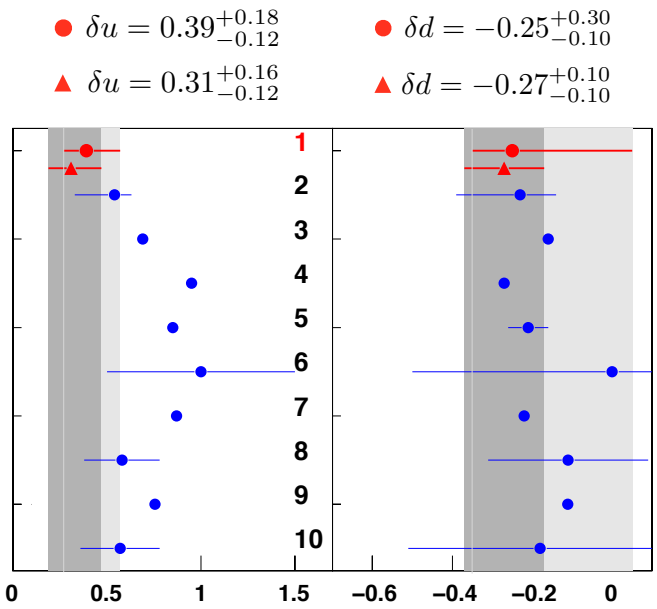

FIG. 8: The tensor charge $\delta q \equiv \int_0^1 dx\,[\Delta_T q(x) - \Delta_T \bar{q}(x)]$ for u (left) and d (right) quarks, computed using the transversity distributions obtained from our best fits, Table II (top solid red circles) and Table III (solid red triangles). The gray areas correspond to the statistical uncertainty bands in our extraction. These results are compared with those given in Ref. [7] (number 2), obtained in Ref. [8] (number 10) and computed with lattice [28] (number 5) or model calculations Refs. [26, 27, 29–32](respectively, numbers 3, 4 and 6-9).

the TMD-evolution of $\Delta_T q(x, k_\perp)$ and $\Delta^N D_{h/q^\uparrow}(z, p_\perp)$. Great progress has been recently achieved in the study of the TMD-evolution of the unpolarized and Sivers transverse momentum dependent distributions [35–39] and a similar progress is expected soon for the Collins function and the transversity TMD distribution [40].

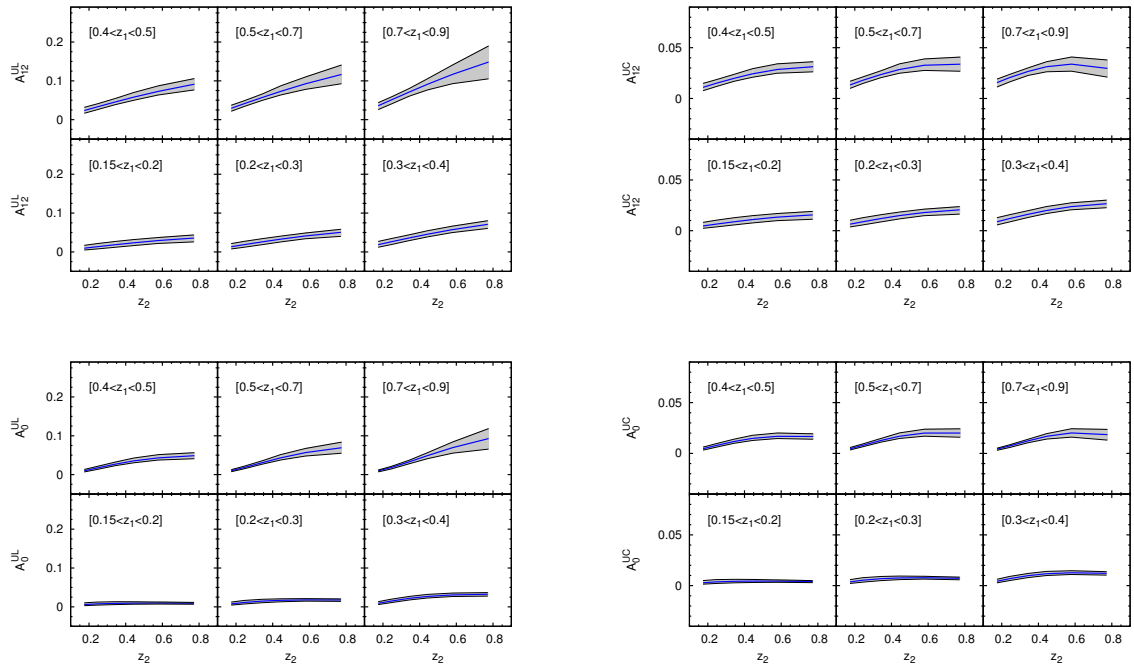

FIG. 9: Estimates, obtained from our global fit, for the azimuthal correlations A_{12}^{UL}, A_{12}^{UC}, A_0^{UL} and A_0^{UC} in unpolarized $e^+e^- \to h_1h_2\,X$ processes at BaBar [25]. The solid lines correspond to the parameters given in Table II, obtained by fitting the A_{12} Belle asymmetry; the shaded area corresponds to the uncertainty on these parameters, as explained in the text.

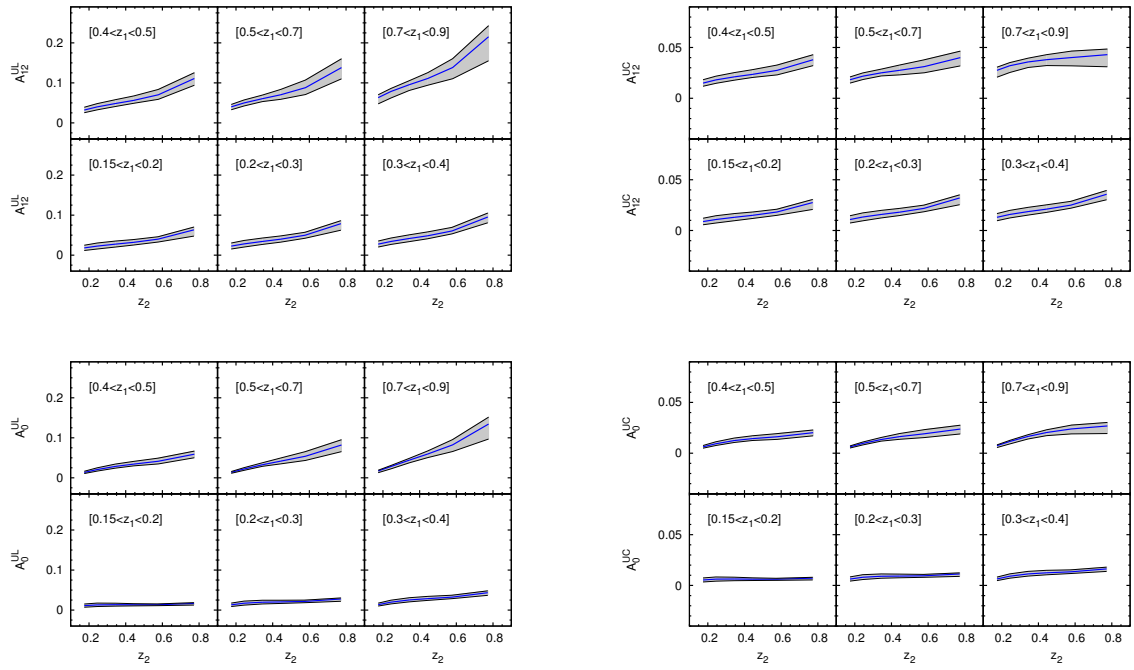

FIG. 10: Estimates, obtained from our global fit, for the azimuthal correlations A_{12}^{UL}, A_{12}^{UC}, A_0^{UL} and A_0^{UC} in unpolarized $e^+e^- \to h_1h_2\,X$ processes at BaBar [25]. The solid lines correspond to the parameters given in Table III, obtained by fitting the A_0 Belle asymmetry; the shaded area corresponds to the uncertainty on these parameters, as explained in the text.

Acknowledgments

Authored by a Jefferson Science Associate, LLC under U.S. DOE Contract No. DE-AC05-06OR23177. We acknowledge support from the European Community under the FP7 "Capacities - Research Infrastructures" program (HadronPhysics3, Grant Agreement 283286). We also acknowledge support by MIUR under Cofinanziamento PRIN 2008. U.D. is grateful to the Department of Theoretical Physics II of the Universidad Complutense of Madrid for the kind hospitality extended to him during the completion of this work.

[1] J. C. Collins, Nucl. Phys. **B396**, 161 (1993).
[2] J. C. Collins, S. F. Heppelmann, and G. A. Ladinsky, Nucl. Phys. **B420**, 565 (1994).
[3] R. Jaffe, X.-m. Jin, and J. Tang, Phys. Rev. Lett. **80**, 1166 (1998).
[4] M. Radici, R. Jakob, and A. Bianconi, Phys. Rev. **D65**, 074031 (2002).
[5] D. Boer and P. Mulders, Phys. Rev. **D57**, 5780 (1998).
[6] M. Anselmino, M. Boglione, U. D'Alesio, A. Kotzinian, F. Murgia, and A. Prokudin, Phys. Rev. **D75**, 054032 (2007).
[7] M. Anselmino, M. Boglione, U. D'Alesio, A. Kotzinian, S. Melis, F. Murgia, and A. Prokudin, Nucl. Phys. Proc. Suppl. **191**, 98 (2009).
[8] A. Bacchetta, A. Courtoy, and M. Radici (2012), arXiv:1212.3568 [hep-ph].
[9] C. Adolph et al. (COMPASS Collaboration), Phys. Lett. **B717**, 376 (2012).
[10] A. Martin (COMPASS Collaboration) (2013), arXiv:1303.2076 [hep-ex].
[11] A. Airapetian et al. (HERMES Collaboration), Phys. Lett. **B693**, 11 (2010).
[12] R. Seidl et al. (Belle Collaboration), Phys. Rev. **D86**, 032011(E) (2012).
[13] M. Anselmino, M. Boglione, U. D'Alesio, S. Melis, F. Murgia, E. Nocera, and A. Prokudin, Phys. Rev. **D83**, 114019 (2011).
[14] A. Bacchetta, M. Diehl, K. Goeke, A. Metz, P. J. Mulders, and M. Schlegel, JHEP **0702**, 093 (2007).
[15] A. Bacchetta, U. D'Alesio, M. Diehl, and C. A. Miller, Phys. Rev. **D70**, 117504 (2004).
[16] M. Anselmino, M. Boglione, U. D'Alesio, A. Kotzinian, F. Murgia, and A. Prokudin, Phys. Rev. **D71**, 074006 (2005).
[17] M. Gluck, E. Reya, and A. Vogt, Eur. Phys. J. **C5**, 461 (1998).
[18] D. de Florian, R. Sassot, and M. Stratmann, Phys. Rev. **D75**, 114010 (2007).
[19] W. Vogelsang, Phys. Rev. **D57**, 1886 (1998).
[20] D. Boer, R. Jakob, and P. J. Mulders, Nucl. Phys. **B504**, 345 (1997).
[21] R. Seidl et al. (Belle Collaboration), Phys. Rev. Lett. **96**, 232002 (2006).
[22] R. Seidl et al. (Belle Collaboration), Phys. Rev. **D78**, 032011 (2008).
[23] M. Anselmino, M. Boglione, U. D'Alesio, E. Leader, S. Melis, F. Murgia, and A. Prokudin, Phys. Rev. **D86**, 074032 (2012).
[24] M. Anselmino, M. Boglione, U. D'Alesio, A. Kotzinian, S. Melis, F. Murgia, A. Prokudin, and C. Turk, Eur. Phys. J. **A39**, 89 (2009).
[25] I. Garzia (BABAR Collaboration) (2012), arXiv:1211.5293 [hep-ex].
[26] I. Cloet, W. Bentz, and A. W. Thomas, Phys. Lett. **B659**, 214 (2008).
[27] M. Wakamatsu, Phys. Lett. **B653**, 398 (2007).
[28] M. Gockeler et al. (QCDSF Collaboration, UKQCD Collaboration), Phys. Lett. **B627**, 113 (2005).
[29] H.-x. He and X.-D. Ji, Phys. Rev. **D52**, 2960 (1995).
[30] B. Pasquini, M. Pincetti, and S. Boffi, Phys. Rev. **D76**, 034020 (2007).
[31] L. P. Gamberg and G. R. Goldstein, Phys. Rev. Lett. **87**, 242001 (2001).
[32] M. Hecht, C. D. Roberts, and S. Schmidt, Phys. Rev. **C64**, 025204 (2001).
[33] X. Qian et al. (Jefferson Lab Hall A Collaboration), Phys. Rev. Lett. **107**, 072003 (2011).
[34] S. Scopetta, Phys. Rev. **D75**, 054005 (2007).
[35] J. Collins, Foundations of perturbative QCD, Cambridge monographs on particle physics, nuclear physics and cosmology, N. 32, Cambridge University Press, Cambridge (2011).
[36] S. M. Aybat and T. C. Rogers, Phys. Rev. **D83**, 114042 (2011).
[37] S. M. Aybat, J. C. Collins, J.-W. Qiu, and T. C. Rogers, Phys. Rev. **D85**, 034043 (2012).
[38] S. M. Aybat, A. Prokudin, and T. C. Rogers, Phys. Rev. Lett. **108**, 242003 (2012).
[39] M. Anselmino, M. Boglione, and S. Melis, Phys. Rev. **D86**, 014028 (2012).
[40] A. Bacchetta and A. Prokudin (2013), arXiv:1303.2129 [hep-ph].